EasyChair Preprint

№ 2220

Effect of Duty Cycle on Flow Induced by a Dielectric Barrier Discharge Plasma Actuator in Burst Mode

B.K. Mishra and Pradipta Panigrahi

December 21, 2019

Proceedings of the 7th International and 45th National Conference on Fluid Mechanics and Fluid Power (FMFP)
December 10-12, 2018, IIT Bombay, Mumbai, India

FMFP2018 - 79

Effect of Duty Cycle on Flow Induced by a Dielectric Barrier Discharge Plasma Actuator in Burst Mode

Bal Krishan Mishra

Department of Mechanical Engineering
IIT Kanpur, Kanpur, U.P., India-208016
Email: bkmishra@iitk.ac.in

P. K. Panigrahi

Department of Mechanical Engineering
IIT Kanpur, Kanpur, U.P., India-208016
Email: panig@iitk.ac.in

Abstract

The periodic vortical flow pattern generated by a burst modulated dielectric barrier discharge plasma actuator in quiescent atmospheric air is presented. The flow field has been studied with the help of smoke flow visualization and time resolved particle image velocimetry techniques. The effect of duty cycle on the behavior of periodic vortex has been presented. The periodic vortex behavior and it's interaction with the remnant vortex have been described with the help of streaklines, vorticity and $Q-$criterion. The duty cycle alters the vortex growth and vortex core location.

Keywords: *DBD plasma actuator; Smoke visualization; Starting vortex; Periodic vortex; Remnant vortex*

I. INTRODUCTION

A Dielectric Barrier Discharge (DBD) plasma actuator is one of the actuators for active flow control. The main advantage of DBD actuator is it's simplicity, lightweight design, low power consumption and fast response. A typical DBD plasma actuator is shown in Figure 1(a). It consists of two electrodes, one of the electrode is exposed to the flow (ambient fluid in case of quiescent condition) and the other electrode is encapsulated. The actuator is operated by a high $\mathcal{O}$(kHz) frequency and high $\mathcal{O}$(kV) voltage Alternating Current (AC) signal. The exposed electrode is connected to high voltage and the encapsulated electrode is grounded. When the actuation is initiated, a strong electric field is created due to presence of high voltage causing the ionization of air present in the neighborhood region of the exposed electrode and consequently, plasma is formed. In the presence of an electric field, ions move in to-and-fro direction from the exposed electrode to the encapsulated electrode. This causes numerous collisions between the charged and uncharged molecules, generating a net positive body force and an overall flow motion is induced towards the encapsulated electrode [1]–[4].

When the actuator is operated in steady or continuous mode by the application of a continuous AC waveform, a starting vortex is generated which later transforms into a wall jet [5]. The starting vortex is the consequence of impulsive nature of the body force at the onset. When it is operated in unsteady or burst mode with a burst signal (burst of AC waveform) the vortical structures are generated periodically and thus, it acts as a periodic vortex generation device and can be used for periodic excitation of flow. A schematic of a typical burst signal of sinusoidal AC waveform is shown in Figure 1(b). The $\phi(t)$ denotes the amplitude of signal which is periodic in time, t with a peak to peak amplitude of ϕ_{pp}. The other parameters of the burst signal are defined as follows: T and $f = 1/T$ is the period and frequency of AC waveform respectively; T_{on} is burst or ON time and T_{off} is idle or OFF time of the burst signal; burst period, $T_b = T_{on} + T_{off}$; burst frequency, $f_b = 1/T_b$; duty cycle, $\alpha = T_{on}/T_b$); and burst ratio, $T_r = T_{off}/T_{on}$.

In several past literatures, e.g. [6]–[8] it has been demonstrated that the DBD plasma actuator operating in the burst mode provides better flow control compared to the continuous mode. These results motivate us to investigate the flow induced by the actuator in quiescent medium by operating the actuator in burst mode. In such a situation, development of periodic vortex has been studied by Mishra and Panigrahi [9] and they observed the third and subsequent vortices are periodic in nature. By extending the past work, the present study has been carried out in a systematic manner to illustrate the effect of α. The actuator is operated in a burst mode and the flow induced by the DBD plasma actuator in quiescent medium have been investigated.

II. METHODOLOGY

A. Experimental setup details

The DBD plasma actuator shown in Figure 1(a) is fabricated on a 165×145 mm^2 printed circuit board (PCB) made of flame retardant–4 (dielectric constant =

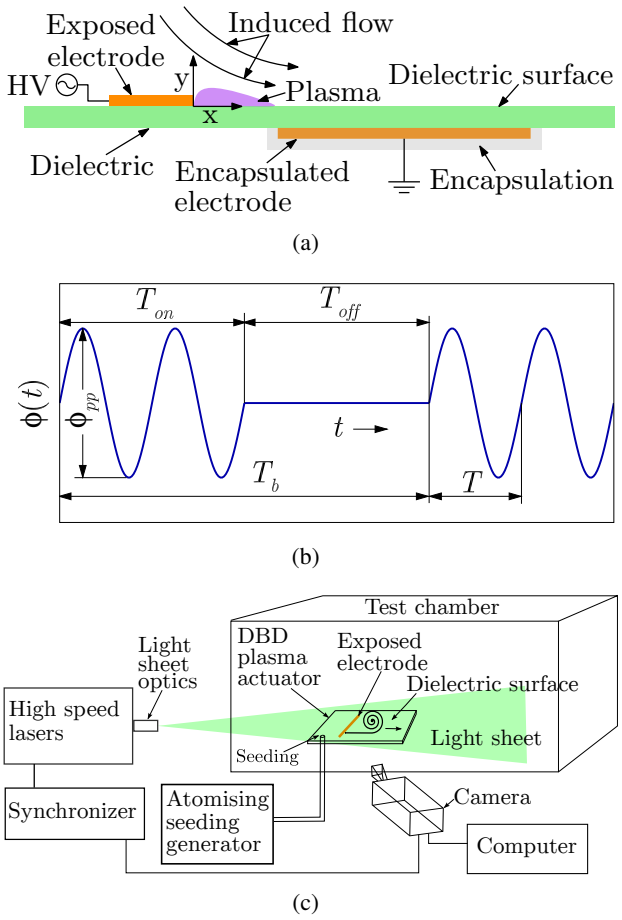

Figure 1: **Schematic of (a) DBD plasma actuator, (b) a burst actuation signal and (c) the experimental arrangement for smoke visualization and TRPIV.**

4.7) by using PCB printing. The dielectric and electrode thickness are 1 mm and 35 μm respectively. The exposed and encapsulated electrodes are 2.5 and 10 mm wide in width respectively with an equal spanwise length of 10 cm. The gap between the exposed and encapsulated electrode is zero. The DBD plasma actuator is operated with a burst signal as shown in Figure 1(b) by using a high speed high voltage amplifier. More detailed information about the experimental facility can be found in authors' previous work [9], [10]. The experiments were carried out at constant actuation parameter of $\phi_{pp} = 14$ kV, $f = 2$ kHz and $f_b = 10$ Hz. The α is varied in a step size of 10% in the range of $50 \leq \alpha \geq 90\%$ (equivalently, $0 < T_r < 1$ and $T_{on} \geq T_{off}$).

B. Measurement technique

The experimental arrangement for smoke visualization and time resolved particle image velocimetry (TRPIV) is shown in Figure 1(c). Both the Smoke visualization and TRPIV are carried out inside a closed rectangular chamber large enough compared to the size of vortical structures. The setup comprises a high speed camera (Phantom v341) equipped with a Nikon 105 f/2.8 lens, a high speed Nd:YAG pulsed laser (Photonics DS-532-10) with beam shaping optics, a synchronizer, a computer and an atomizing seeding generator. The images are recorded in a cine format at 2500 frames per second with a resolution of 1280×920 pixel^2 which is equal to 64×46 mm^2 in real units. The smoke visualization and TRPIV measurements are carried out on the same setup but separately and by using separate but identical actuators. The smoke and seeding particles are generated by the atomizing seeding generator by using Dioctyl Sebacate ($C_{26}H_{50}O_4$). For the visualization, smoke is supplied with the help of a nozzle at the upstream of the actuator. The images for TRPIV measurements were acquired by filling the entire test chamber with seeding particles.

The post processing of TRPIV images are carried out using VidPIV software from Oxford Lasers. A cross-correlation scheme is applied on an interrogation window size of 64×64 pixel^2 with 50% overlap. The cross-correlated images are filtered by local velocity filters and subsequent outliers were interpolated. The interrogation widow is reduced to a size of 32×32 pixel^2 and an adaptive cross-correlation scheme is applied with 50% overlap. Local velocity filters followed by interpolation of outliers are further used to generate the final vector map.

III. RESULTS AND DISCUSSION

Figure 2 show the instantaneous smoke visualization images of the periodic vortex induced by the DBD plasma actuator for five different values of burst parameter, α at $t/T_b = 0.5$. The absolute time, t is equal to 50 ms and the time, t is taken zero at the start of the burst cycle. The smoke visualization presented in Figure 2 show the streaklines of the induced flow. The location of vortex core and vortex separation point are marked with a + sign and $\triangledown$ symbol respectively in each visualization image. The vortex generated in the current burst cycle is called as periodic vortex and the vortex generated in preceding burst cycle is called as remnant vortex and are labeled in Figure 2 at $\alpha = 60\%$. The visualization images reveal that α has an overall influence on vortex core location, vortex separation location and nature of remnant vortex. Corresponding to smoke visualization shown in Figure 2 the phase averaged vorticity and $Q-$criterion (the second invariant of velocity gradient tensor which identify the vortices with their positive values) are calculated from the TRPIV measurements and are presented in Figure 3. The $Q-$criterion is calculated for the precise location of the core. The phase averaged results are obtained

from an ensemble of 9 TRPIV snapshots, conforming the repeatability of vortical structures in each burst cycle. It is found that the smoke visualization and TRPIV results are in good support with each other which conforms the reproducibility of the flow pattern. It may be noted that, two separate but identical actuators has been used for TRPIV and smoke visualization experiments.

The smoke visualization shown in Figure 2 and $Q-$criterion results shown in Figure 3 reveals that the core location is a function of burst parameter, α. For a greater value of α, T_{on} is more and consequently, the actuator remains ON for a long time interval due to which more momentum transfer takes place that results in an increased value of maximum induced velocity. The shape of periodic vortex changes at high values of α due to strong interaction between periodic vortex and remnant vortex compared to the low values of α (see, visualization at α = 50 and 90% in Figure 2). The behavior of remnant vortex is also found to be different at different values of α which is explicit from the contour lines of the vorticity shown in Figure 3. The TRPIV results of vorticity show the presence of both primary (positive) and secondary (negative) vorticity. The secondary vorticity (it's not a vortex as no positive value of Q exists for that region) is found underneath the periodic vortex after the separation point. By the roll up of the periodic vortex, secondary vorticity is stretched and gets wrapped around the periodic vortex. Similar behavior of secondary vorticity has been observed by Whalley and Choi [11] when a starting vortex is formed.

The effect of α on the periodic vortex core location, x_c and y_c is shown in Figure 4. The x_c and y_c are the core location in x and $y-$direction respectively, labeled in Figure 3 at α = 60%. The x_c increases and y_c decreases with increase in α. Overall, these results suggest that the amount of momentum addition to the main flow and spatial distribution of the added momentum are function of burst parameter, α which can have greater influence in flow control application.

IV. CONCLUSIONS

The overall nature of the general flow pattern generated by the DBD plasma actuator is a function of burst parameter. The maximum magnitude of induced velocity increases with increase in values of α. This change is attributed to different amount of momentum addition for different values of duty cycle, α. The change in induced velocity modifies the flow behavior in two ways: (1) the interaction between the periodic and remnant vortex and (2) the growth and development of the vortex. It is concluded that DBD plasma actuator can generate variety

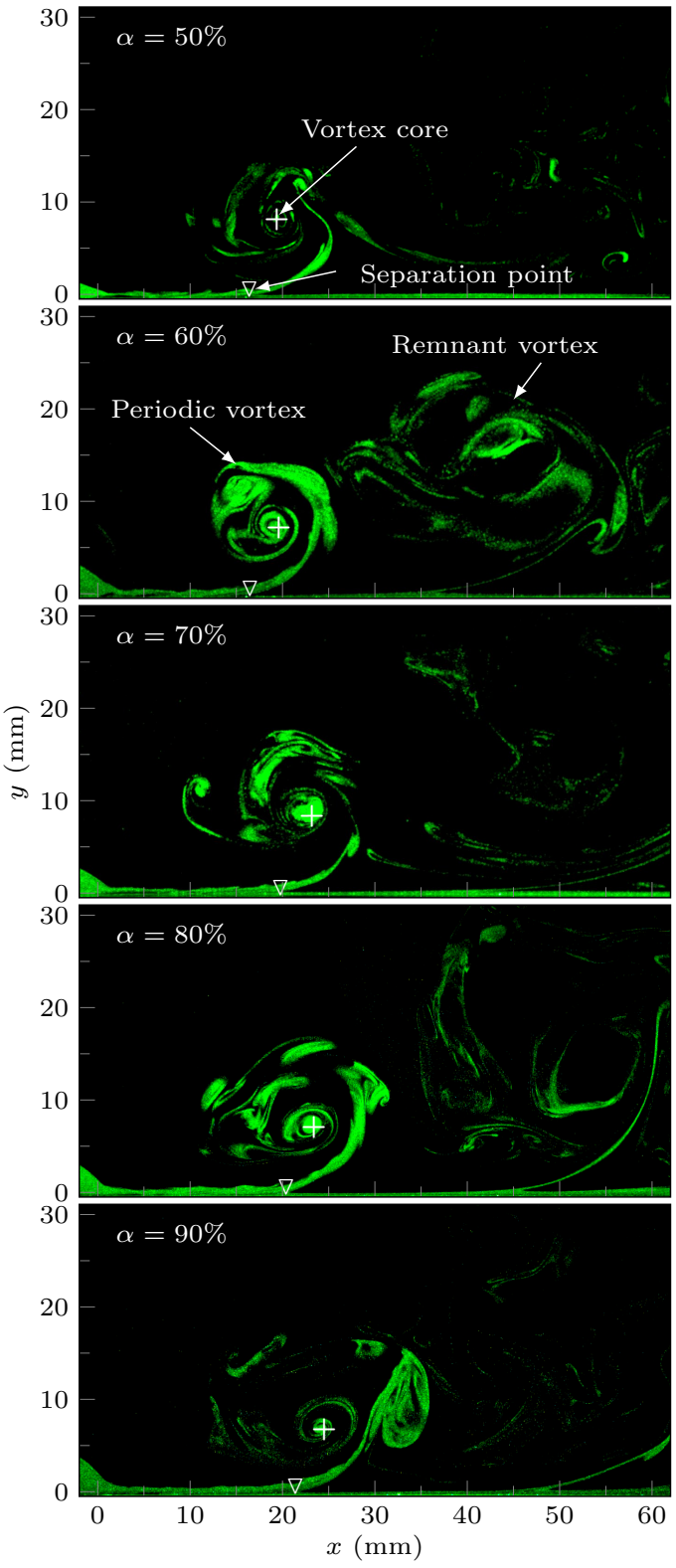

Figure 2: **Instantaneous smoke visualization of flow induced by DBD plasma actuator in burst mode operation at $t/t_b = 0.5$ ($t = 50$ ms) with increasing duty cycle, α. The time $t = 0$, corresponds to start of the burst cycle. The actuator is operated at constant values of $\phi_{pp} = 14$ kV, $f = 2$ kHz and $f_b = 10$ Hz.**

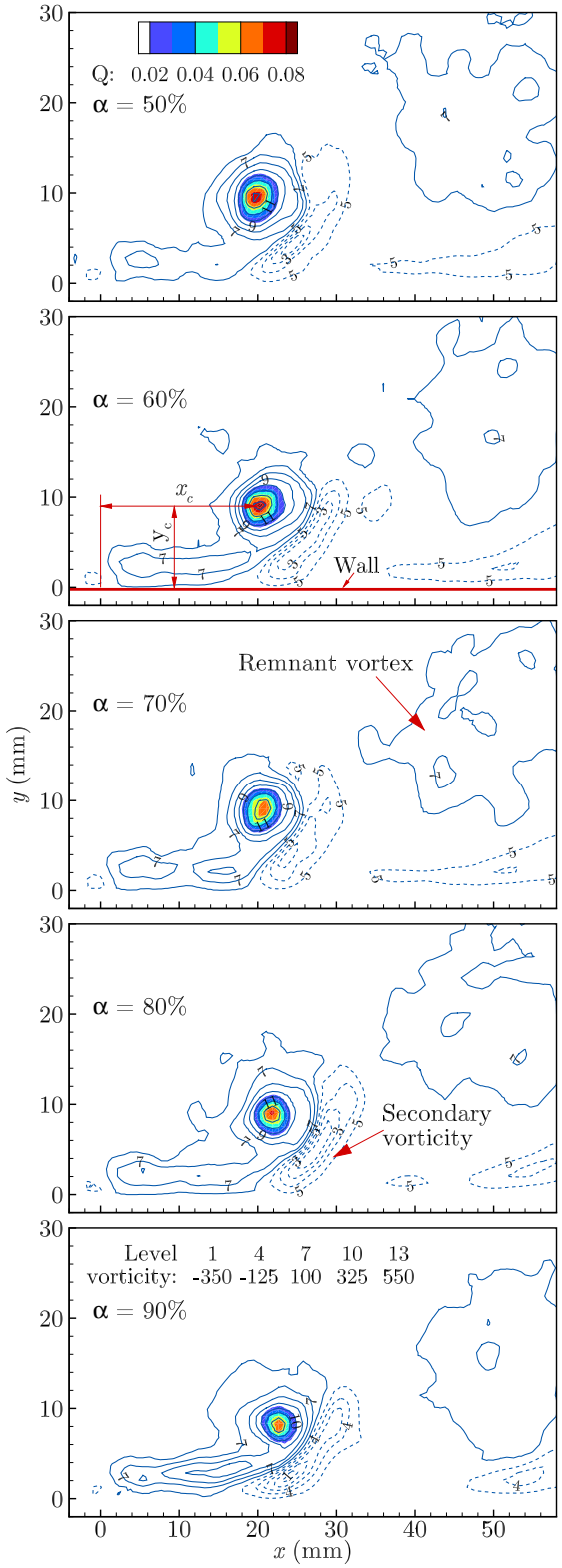

Figure 3: **The phase averaged vorticity field and Q−criterion for the identification of vortex core corresponding to Figure 2. The vorticity contour lines are superimposed over the filled color contours of Q−criterion. The solid (dashed) line corresponds to positive (negative) vorticity.**

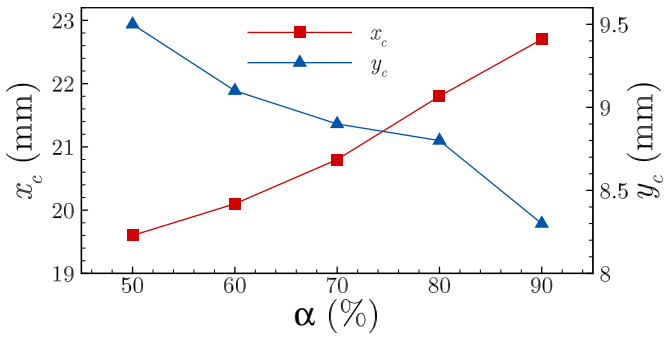

Figure 4: **Effect of duty cycle, α on the core locations, $\mathbf{x_c}$ and $\mathbf{y_c}$ of periodic vortex. The core locations are extracted from the phase averaged TRPIV results shown in Figure 3.**

of flow patterns in burst mode for an effective flow control in various applications.

References

[1] E. Moreau, "Airflow control by non-thermal plasma actuators," *Journal of Physics D: Applied Physics*, vol. 40, no. 3, pp. 605–636, 2007.

[2] B. K. Mishra and P. K. Panigrahi, "Design and characterization of a novel dielectric barrier discharge plasma actuator for flow control application," in *Fluid Mechanics and Fluid Power – Contemporary Research*. Springer India, 2016, pp. 1545–1554.

[3] J. Gregory, C. Enloe, G. Font, and T. McLaughlin, "Force production mechanisms of a dielectric-barrier discharge plasma actuator," in *45th AIAA Aerospace Sciences Meeting and Exhibit*. AIAA, 2007.

[4] J. R. Roth, D. M. Sherman, and S. P. Wilkinson, "Electrohydrodynamic flow control with a glow-discharge surface plasma," *AIAA Journal*, vol. 38, no. 7, pp. 1166–1172, 2000.

[5] T. N. Jukes, "Turbulent drag reduction using surface plasma," Ph.D. dissertation, University of Nottingham, 2007.

[6] N. Benard, J. Jolibois, and E. Moreau, "Lift and drag performances of an axisymmetric airfoil controlled by plasma actuator," *Journal of Electrostatics*, vol. 67, no. 2-3, pp. 133–139, 2009.

[7] Y. hong Li, Y. Wu, M. Zhou, C. bing Su, X. wei Zhang, and J. qiang Zhu, "Control of the corner separation in a compressor cascade by steady and unsteady plasma aerodynamic actuation," *Experiments in Fluids*, vol. 48, no. 6, pp. 1015–1023, 2009.

[8] K. Asada and Y. Ninomiya, "Airfoil flow experiment on the duty cycle of DBD plasma actuator," in *47th AIAA Aerospace Sciences Meeting including The New Horizons Forum and Aerospace Exposition*, vol. 531. AIAA, 2009.

[9] B. K. Mishra and P. K. Panigrahi, "Formation and characterization of the vortices generated by a DBD plasma actuator in burst mode," *Physics of Fluids*, vol. 29, no. 2, p. 024104, 2017.

[10] ——, "Repeating vortices induced by the dielectric barrier discharge plasma actuator," in *Fluid Mechanics and Fluid Power – Contemporary Research*, 2016.

[11] R. D. Whalley and K.-S. Choi, "The starting vortex in quiescent air induced by dielectric-barrier-discharge plasma," *Journal of Fluid Mechanics*, vol. 703, pp. 192–203, 2012.